BABEŞ-BOLYAI UNIVERSITY CLUJ-NAPOCA

FACULTY OF PHYSICS

Camelia Lehene

Vibrational spectroscopic studies on complex molecular systems used as food additives

PhD Thesis Summary

Scientific supervisor: Prof. Dr. Onuc Cozar

Cluj-Napoca

2011

CONTENTS

Keywords:

- IR, Raman, SERS, DFT
- food addittives
- sodium benzoate
- monosodium glutamate (MSG)
- annatto
- bixin, norbixin

INTRODUCTION

Raman spectroscopy is nowadays steadily gaining on importance for online monitoring of chemical reactions, analysis of food, pharmaceuticals and chemicals, and increasingly for many other real-world applications. Raman spectroscopy yields detailed informations about molecular vibrations. As molecular vibrations are very sensitive to strength and types of chemical bonds, Raman spectroscopy is useful not only in identifying molecules but also in shedding light on molecular structures. In addition, Raman spectra also reflect changes in the molecules and thus they are surroundings helpful in studying intra- and intermolecular interactions.

Surface-enhanced Raman spectroscopy (SERS) is a powerful technique for the sensitive and selective detection of low-concentration analytes.

Theoretical calculations allow a complete assignment of experimental obtained Raman spectra [Chi07]. Molecular electrostatic potential (MEP) is related to the electronic density and is a very useful descriptor in understanding sites for electrophilic attack and nucleophilic reactions as well as hydrogen bonding interactions.

Food additives are some of the latest provocation in nutrition. These substances are intentionally added to foodstuffs to perform certain technological functions, for example to colour, sweeten or preserve.

The thesis is structurated in four chapters. The first chapter presents some theoretical aspects on the methods used in the experimental investigations: **IR, Raman and SERS spectroscopy.**

Chapters two, three and four are dedicated to physico-chemical characterization of three substances used as food additives.

The theme of the second chapter is the physico-chemical characterization of the sodium benzoate molecule. The chemical formula for sodium benzoate is $NaC_6H_5CO_2$, with E number **E 211**. Sodium benzoate is a widely used food preservative and is the sodium salt of benzoic acid; it exists in this form when dissolved in water. It is the product result of the reaction between sodium hydroxide and benzoic acid. Under acidic conditions it is bacteriostatic and fungistatic. This salt is most commonly used in acidic foods such as salad dressings (vinegar), carbonated drinks (carbonic acid), jams and fruit juices (citric acid), pickles (vinegar) and condiments. It is

also used as a preservative in medicines and cosmetics. In combination with ascorbic acid (vitamin C, E 300), sodium benzoate is a known carcinogen.

The third chapter containts some original results obtained by studying the sodium glutamate molecule **E 621**. This study is a combination of experimental results gained by vibrational spectroscopic methods with theoretical results based on the DFT formalism. Monosodium glutamate (MSG), the sodium salt of glutamic acid, is probably the most common food additive used in many packaged and prepared foods. MSG is a neurotoxin and it is employed to give a "meaty", "savory" or "brothy" taste to foods by stimulating the glutamate receptors on the tongue. It causes the taste of *umami*, one of the five basic flavors besides salts, sweet, bitter and sours [Wei84]. MSG is a fine white crystal substance that looks like salt. Other synonyms of MSG are: L-glutamic acid, monosodium salt, hydrolyzed vegetable protein, autolyzed yeast, and whey protein.

Monosodium glutamate, is a salt of glutamic acid. Glutamic acid is one of the 20 amino acids making up proteins.

The fourth chapter is dedicated to the study of an important dye used in industry [Ram10], annatto**, E 160b**. Annatto (Orlean, Terre orellana, L. Orange, Natural Orange 4, E 160b) is a natural orange/yellow coloring from the carotenoids class, extracted from the outer coats of the seeds of the tropical shrub Bixa-Orellana-L [Bit05]. The carotenoid bixin represents more than 80% of the total carotenoids found in the outer coat of the seeds. Norbixin is the dicarboxylic acid and water-soluble form of bixin [Dia11]. These dyes are widely used in foods and they find their applications in cheese, butter, sausages, ice cream, meat, etc. [Sil08]. Other applications include formulation of drugs and cosmetics [Alv06]. Nowadays, the synthetic dyes and the natural dyes are indispensable for food, pharmaceutical and cosmetics applications. As color is often a key consumer perception for food preference and acceptability, alimentary dyes play a key factor in the food industry [Bit05].

The search of new techniques that can be applied in the analysis of natural products without unduly interfering with their structure represents a new trend in the field of food research [Bit05].

Chapter II. Physico-chemical characterization of the sodium benzoate molecule – E 211

The molecular structure of the sodium benzoate molecule is presented in Figure II.1.a. Benzoate exists in a pH-dependent equilibrium between uncharged acid molecules and charged anions. The pK_a value of benzoate is 4.2.

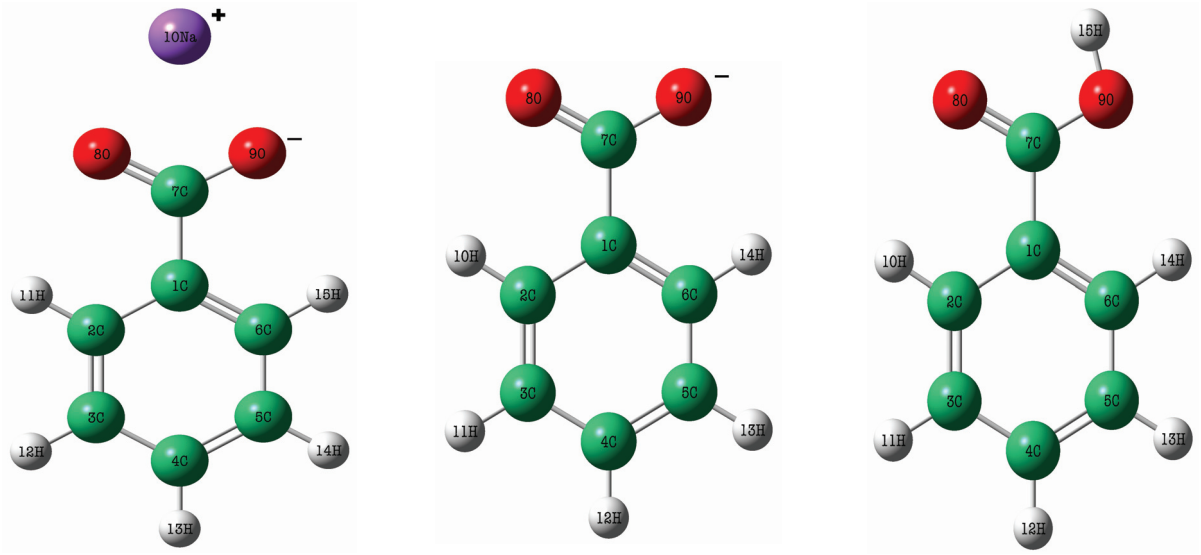

(a) **(b)** **(c)**

Figure II. 1. Molecular structure (a), unprotonated form (b), and neutral form (c) of sodium benzoate

II. 1 Experimental and theoretical methods

Sodium benzoate, $C_7H_5NaO_2$, (purity 99 %) was purchased from Aldrich. We used pure and commercially available sodium benzoate for our measurements. On behalf of the commercially available sodium benzoate no analytical purity certificate was accessible. In most cases, impure ingredients are used by many companies. For the SERS measurements, silver colloid, prepared according to the literature [Lee82], was used as metallic substrate. The SERS samples were obtained by adding 0.1 ml of sodium benzoate solutions at different concentrations into 3.5 ml silver colloid, getting the final SERS concentrations ($2.8x10^{-3}$ – $2.8x10^{-4}$ M). The pH values were adjusted by adding HCl or NaOH solutions (10^{-1} M), respectively.

The FT-Raman spectrum was obtained by using a Bruker IFS 120HR spectrometer with an integrated FRA106 Raman module and a resolution of 1 cm^{-1}. The 1064 nm radiation from an Nd-YAG laser with an output of 1 W was employed for the excitation. A Ge detector operating at liquid nitrogen temperature was used and the number of scans was 1000.

The micro-Raman and SERS spectra on silver colloid were recorded with a Dilor Labram spectrometer using the 514.5 nm excitation lines from a Spectra Physics argon ion laser. The spectra were collected in the back-scattering geometry with a resolution of 2 cm^{-1}. The detection of Raman signal was carried out with a CCD camera (Photometric model 9000), while the laser power varied from 100 to 250 mW as it is indicated for each figure caption.

The molecular geometry optimizations (Fiure II.1.) and theoretical frecquencies were performed with the Gaussian 03 software package [Gau03] by using DFT methods with B3LYP functionals.

II.2 Raman spectra of polycrystalline sodium benzoate

Comparing the FT-Raman spectrum (Figure II.2.a) of pure sodium benzoate with both micro-Raman spectra of impure (industrial) (Figure II.2.b) and pure (Figure II.2.c) sodium benzoate, respectively, one can observe the similarities in band positions and relative intensities.

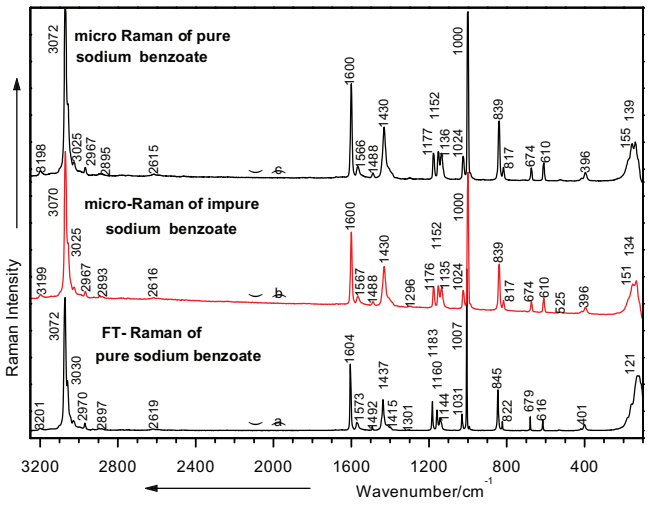

Figure II.2. FT-Raman spectrum of pure (a) micro-Raman spectra of industrial (b) and pure (c) sodium benzoate. Excitations: 1064 nm, 1 W (a); 514.5 nm, 25 mW (b); 514.5 nm, 100 mW (c).

Only a weak background, most probably due to fluorescent impurities of the commercial benzoate, is shown by the micro-Raman spectrum of impure sodium benzoate.

All bands may be divided into two groups: bands connected with the carboxylate anion vibrations and bands associated with the aromatic ring vibrations. The medium peak at 1415 cm^{-1} was assigned to the symmetrical stretching mode of the carboxylate anion $\nu_s(COO^-)$.

It can be seen that the bands connected to the aromatic ring vibrations are the very weak band at 3201 cm^{-1} and the very strong band at 3072 cm^{-1}, which were attributed to the aromatic C-H stretching modes. The following bands of the FT-Raman spectrum at 1183, 1160, 1144, and 1031 cm^{-1} are due to the in plane C-H deformation of the benzene ring. Moving forward, the very strong band at 1007 cm^{-1} can be attributed to the breathing mode of the aromatic ring [Boe90, Baj97]. The medium strong band at 1604 cm^{-1} was attributed to stretching mode of the aromatic ring

In conclusion, the FT-Raman and/or the micro-Raman spectra of the pure and impure sodium benzoate can be employed to give-away the marker bands of the sodium benzoate molecule.

II.3 Raman spectrum of the sodium benzoate solution

On passing from the FT-Raman spectrum of sodium benzoate in polycristaline state to the micro-Raman spectrum of the sodium benzoate solution, several changes in band positions and relative intensities can be observed.

Mainly, the benzoate anion can interact through hydrogen bonds with the water molecules. As a result, these interactions will furnish an important contribution to the sum of all interactions in the benzoate molecule as showed in the spectral shape.

The band corresponding to the symmetric stretching mode of the carboxylate anion, 1383 cm^{-1} in the Raman spectrum of the pure sodium benzoate solution (Figure II.3.b) demonstrates that the anionic form of sodium benzoate is present in solution.

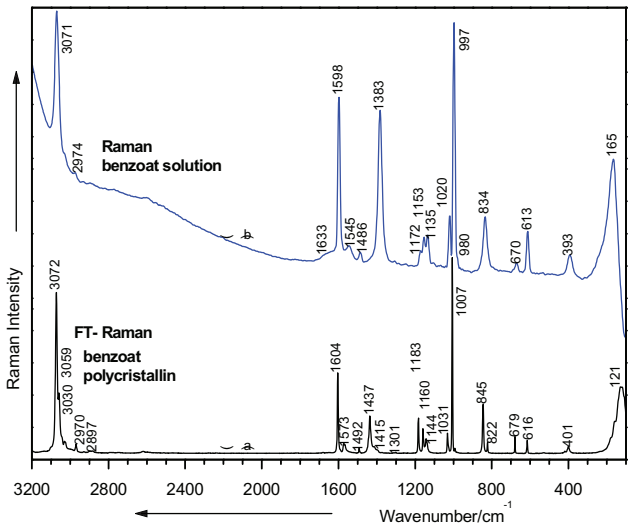

Figure II. 3. FT-Raman spectrum of the solid state sodium benzoate (a) and Raman spectrum of the 1 M sodium benzoate solution (b). Excitation: 1064 nm, 1 W (a); 514.5 nm, 200 mW (b).

II.4 Raman spectra of sodium benzoate solution at different concentrations

The Raman spectra of the sodium benzoate solution were recorded in the concentrations range 1 to 10^{-2} M, from where the Raman signal becomes very weak (Figure II.4).

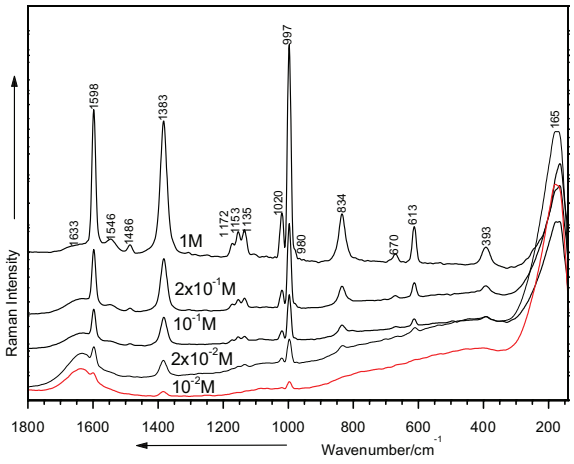

Figure II.4. Micro-Raman spectra of pure sodium benzoate solution at different concentrations. Excitation: 514.5 nm, 200 mW.

II.5 Raman spectra of sodium benzoate solutions at different pH values

By analyzing the micro-Raman spectra of sodium benzoate solutions at different basic (Figure II. 5.) and acid (Figure II. 6.) pH values, we can conclude that the spectra show the transition from the anionic molecular form to the undissociated molecular form of the benzoate molecule.

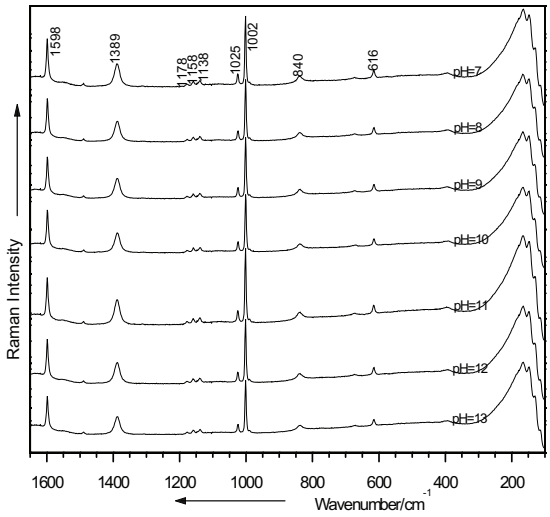

Figure II. 5. Micro-Raman spectra of 10^{-1} M sodium benzoate solution at different basic pH values. Excitation: 514.5 nm, 100 mW.

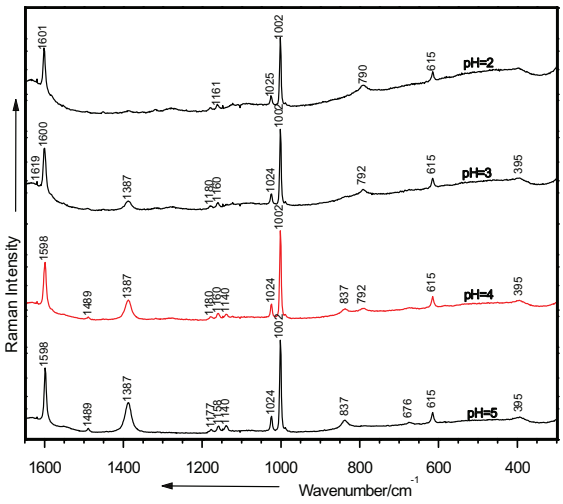

Figure II. 6. Micro-Raman spectra of 10^{-1} M sodium benzoate solution at different acid pH values. Excitation: 514.5 nm, 100 mW.

At basic pH values no important structural changes can be observed in the pH range 7-13, the spectra being attributed to the anionic molecular form of benzoate.

The major changes in band profiles and relative intensities appear below pH=5. On passing from neutral to acid pH values, the bands due to the carboxylate anion stretching modes decrease in relative intensities and become broader (1598, 1387 cm^{-1}). Most likely at pH=4 (pKa=4.2), anionic molecular forms of benzoate coexist in the solution with neutral molecular forms of benzoate. At pH=3, the peak at 1387 cm^{-1} shows a reduced intensity compared to higher pH values, indicating a reduced number of benzoate molecules in the anionic form.

II.6 SERS spectrum of sodium benzoate

The SERS spectrum of sodium benzoate is presented in Figure II. 7 compared to the Raman spectrum of the sodium benzoate solution at micro-molar concentration and pH 7.

.

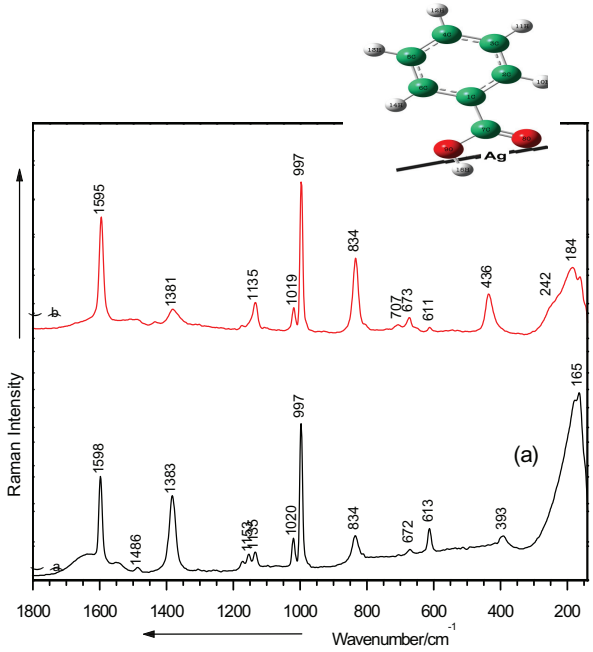

Figure II. 7. Comparison between (a) micro-Raman ($2x10^{-1}$ M) and (b) SERS ($2.8x10^{-3}$ M) spectrum of sodium benzoate (pH 7). Excitation: 514.5 nm, 200 mW (a,b).

On passing from Raman to SERS spectrum at micro-molar concentration, large differences are present in band positions and relative intensities. Since the SERS signal is concentration sensitive, in order to discuss the adsorption behavior of the benzoate to the silver

particles, the SERS spectrum at micro-molar concentration was chosen here for the adsorption geometry proposal

Theoretically, the benzoate molecule could interact with the silver colloidal surface through the carboxylate functional group, or through the π electrons of the benzene ring. The latter supposition is excluded because the breathing vibrational mode of the benzene ring is very high in relative intensity in the SERS spectra, so that a flat orientation to the silver surface is excluded by SERS selection rules [Peic07].

On the other hand, the possibility for benzoate to chemisorb is provided by the presence of the lone electron pairs of oxygen atom from the carboxylate (Figure II.1). In this case, according to the surface selection rules [Baj97] the stretching modes of the carboxylate are expected to be enhanced [Leo04].

The observed bands in the SERS spectrum (Figure II.7) support our consideration. Even more, the intense band at 1595 cm^{-1} assigned to the symmetrical stretching mode of the carboxylate seems to be in the close vicinity of the silver particles with a perpendicular orientation of the ring.

II.7 SERS spectra at different concentrations

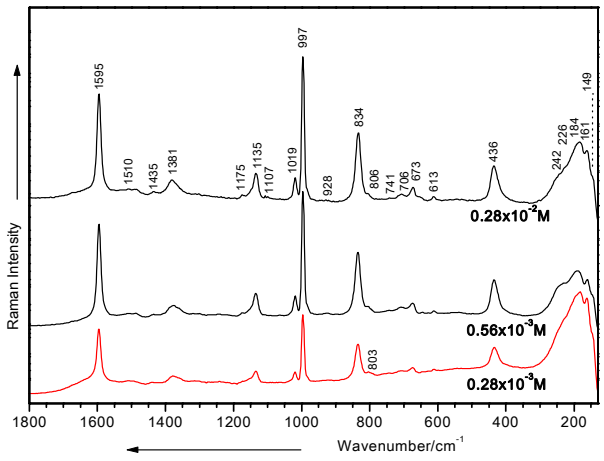

Figure II. 8. SERS spectra of sodium benzoate at different concentrations. Excitation: 514.5 nm, 200 mW.

Lowering the concentration (Figure II.8) several bands decrease in SERS intensity. A strong chemical interaction of sodium benzoate with the silver colloidal particles was also observed at lower concentration through the carboxylate anion.

CONCLUSIONS

FT-Raman and/or micro-Raman spectra of the pure and impure sodium benzoate show bands assigned to the carboxylate anion vibrations and to the aromatic ring vibrations.

Comparing the Raman spectra of sodium benzoate in polycristaline state and in solution, a widening of the bands was observed due to the solvent effect. It was also observed in the Raman spectrum of sodium benzoate solution a new band (1383 cm^{-1}) due to the deformation vibration in the carboxylate group.

The Raman spectra of the sodium benzoate solution were recorded in the concentrations range of 1 to 10^{-2} M, from where the Raman signal becomes very weak

The major changes in the band profiles and relative intensities appear below pH=5 in the Raman spectra of the sodium benzoate. Most likely for pH=4 (pKa=4.2), anionic molecular forms of benzoate coexist in the solution with neutral molecular forms of benzoate.

A strong chemical interaction of sodium benzoate with the silver colloidal particles was observed through the lone pair electrons of the oxygen atoms of the carboxylate anion in a perpendicular orientation.

SERS spectra of sodium benzoate could be recorded even at low concentrations with a conventional SERS setup ($2.8x10^{-4}$ M).

Chapter III Physical-chemical characterization of the monosodium glutamate molecule (E 621)

Monosodium glutamate (E 621) is a common flavor enhancer since nearly a century. Its main component is the amino acid glutamic acid or glutamate. MSG or E 621, the sodium salt of glutamic acid, is probably the most common food additive used in many packaged and prepared foods. Figure III.1. presents atom type of the different isoelectric forms of acid glutamic.

Other synonyms of MSG are: L-glutamic acid monosodium salt, hydrolyzed vegetable protein and whey protein. MSG is a neurotoxin and employed to give a “meaty”, “savory”, or “brothy” taste to foods by stimulating the glutamate receptors on the tongue. It causes the taste of *umami*, one of the five basic flavors besides salts, sweet, bitter, and sour.

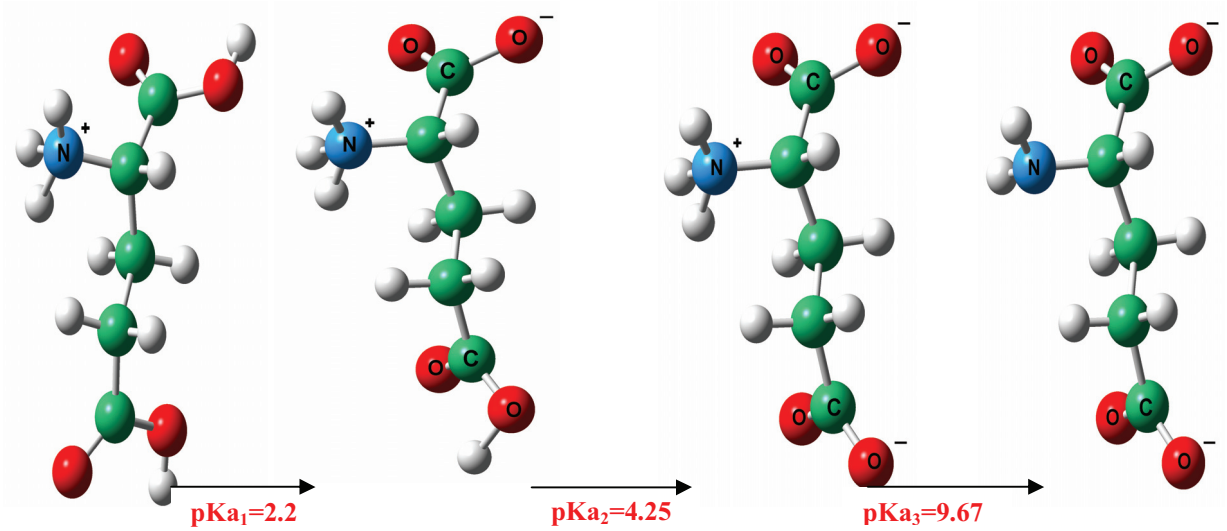

Figure III.1. The isoelectric forms of glutamic acid: (a) the isoelectric form (+1), (b) the isoelectric form (0) or zwitterion form; (c) the isoelectric form (-1); (d) the isoelectric form (-2); determinated by the three values of pKa-s.

III. 1 Experimental and theoretical methods

Commercially available MSG was used in our measurements, for which no analytical purity certificate was accessible. MSG aqueous solutions with concentrations between 10^{-2} M and 1 M were prepared. The pH was adjusted by adding HCl or NaOH solutions (10^{-1} M), respectively.

An UV–VIS–NIR spectrophotometer (Perkin–Elmer Lambda 19) was used for recording the electronic absorption spectra of the samples with a scan speed of 240 nm min^{-1}.

FT-Raman spectra were obtained with a Michelson interferometer (Bruker, IFS 120HR) with an integrated Raman module (Bruker, FRA106). The 1064 nm radiation from a Nd-YAG laser with ca. 1000 mW on the sample was employed for the excitation. A Ge detector operating at liquid nitrogen temperature was used. The interferograms were recorded at a spectral resolution of 1 cm^{-1} with 500 scans.

The Raman and SERS spectra on silver colloid were recorded with a Raman microspectrometer (Horiba-Jobin-Yvon, LabRam model) using the 514.5 nm excitation line from an argon ion laser (Spectra Physics, model 2016). The spectra were collected in the backscattering geometry with a resolution of 5 cm^{-1}. The spectral dispersed Raman signal was detected with a Peltier-cooled CCD camera. The laser power on the sample used in our measurements was 200 mW.

Both geometry optimizations and normal mode calculations were performed with the Gaussian 03 program [Gau03]. Becke's standard exchange functional (B) [Lee88] and Becke's three-parameter hybrid exchange functional (B3) [Bec92] in combination with Perdew and Wang's gradient-corrected correlation functional (PW91) [Per91, Per92] and the correlation functional of Lee, Yang and Parr (LYP) [Bec93] were employed in the DFT calculations. Two different basis sets were used: the 6-311++G** Pople split valence basis set and the LANL2DZ basis set. The LANL2DZ basis set [Dun76] was chosen for extending the calculations at the same level of theory to MSG adsorbed on a silver surface.

III.2 Geometry Optimization

The molecular structure of MSG is presented in Figure III.2.a. The molecular geometry optimizations (Figure III.2. (b) and (c)) and the normal mode calculations were performed by using DFT calculations [Chi05] .

The geometry of MSG was computed and optimized for the first time with the BPW91/6-311++G**, BPW91/LANL2DZ, B3LYP/6-311++G**, and B3LYP/LANL2DZ methods. We demonstrated that both forms of MSG (monohydrate and anhydrous) possess different geometries that can be explained by the molecule protonation possibilities.

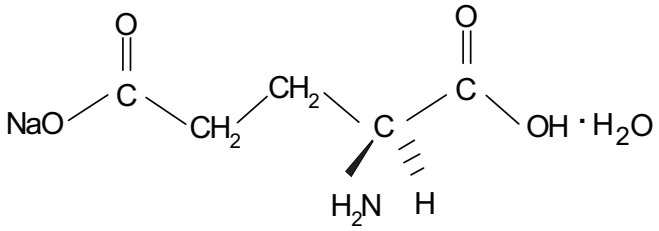

(a)

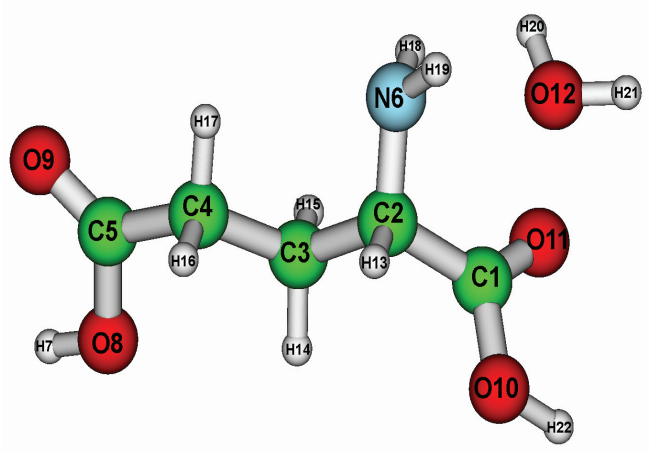

(b)

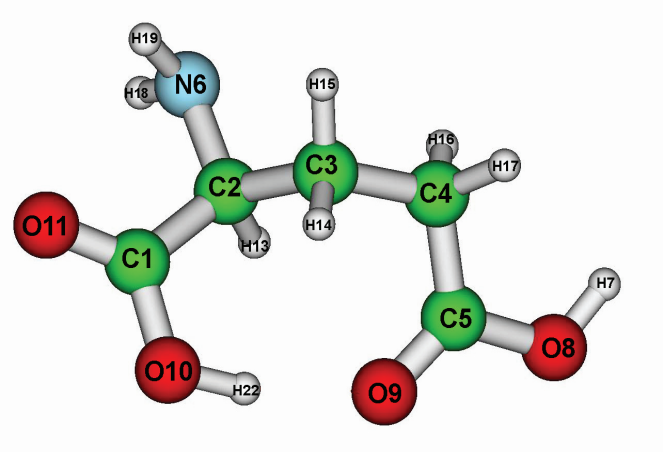

(c)

Figure III.2. Molecular structure (a), B3LYP/LANL2DZ optimized geometry of MSG monohydrate (b), and anhydrous MSG (c).

Theoretical calculations allow a complete assignment of the experimental obtained Raman spectra [Chi07].

III.3 FT-Raman spectrum of solid polycrystalline MSG

Figure III.3.b displays the fingerprint region from 1700-150 cm^{-1}. The very weak peak at 1682 cm^{-1} is due to the stretching mode of C=O bond of the carboxyl groups. The weak band at 1637 cm^{-1} is assigned to the asymmetrical bending mode of the NH_3^+ group, whereas the weak peak at 1624 cm^{-1} corresponds to the asymmetrical stretching mode of the COO^- groups. The adjacent weak peak at 1604 cm^{-1} is attributed to the NH_3^+ deformation mode and the another one at 1571 cm^{-1} to the COO^-Na^+ stretching mode.

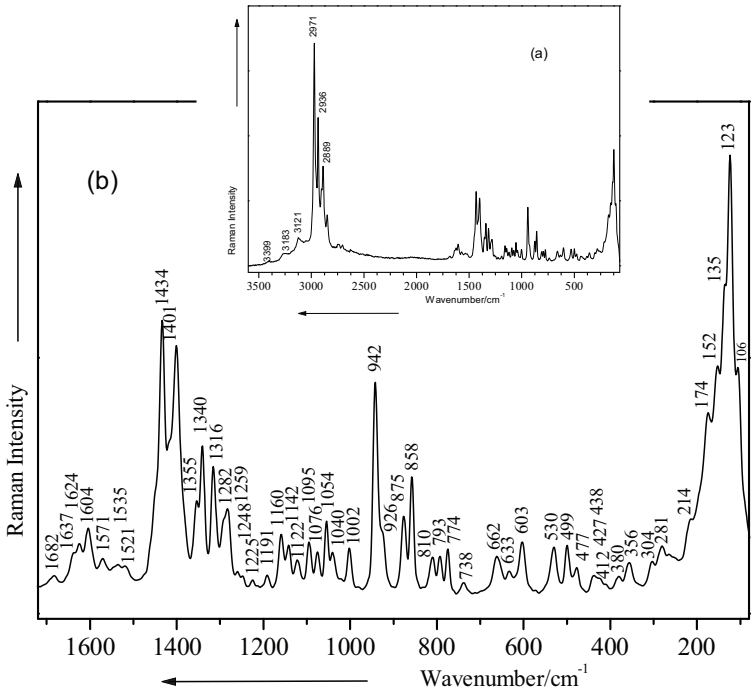

Figure III.3. FT-Raman spectrum of MSG: 3600-68 cm^{-1} (a) and 1700-100 cm^{-1} spectral regions. Excitation: 1064 nm, 1000 mW.

The C–C stretching modes are also observed at 1002 and 942 cm^{-1} and suggest the completely ionized form of MSG as well as all band positions [Dol74].

Because the characteristic bands of the zwitterion structure are present in the Raman spectrum, the presence of the zwitterion structure of the MSG molecule in solid state is also evidenced [Pei07].

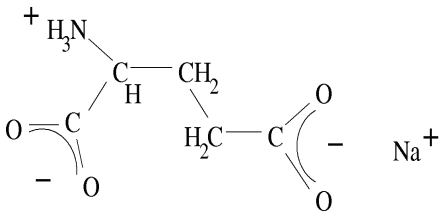

Figure III.4. The zwitterion form of the MSG molecule

III.4 Raman spectroscopy of MSG solutions

Comparing the Raman spectra of MSG in solution with the FT-Raman spectrum of MSG in the solid state (Figure III.5.), one can notice a weaker background, with the relative intensities of the bands slightly changed.

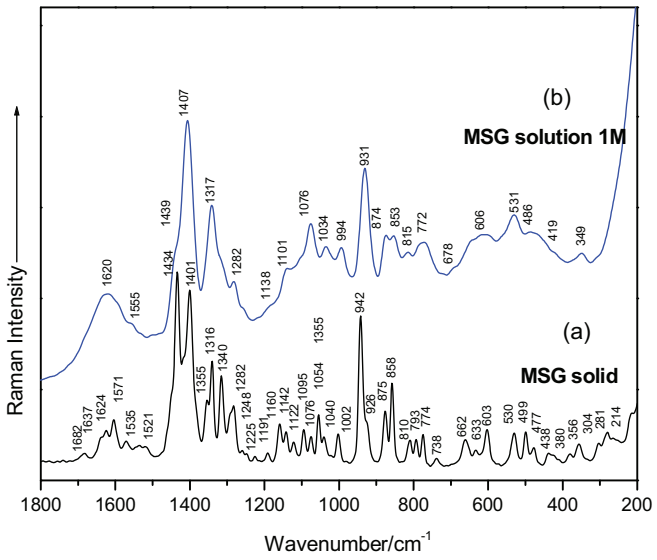

Figure III.5. FT-Raman spectrum of solid polycrystalline MSG (a) compared to Raman spectrum of MSG in aqueous solution 1 M concentration (b). Excitation: 1064 nm, 1000 mW;

An increased intensity of the symmetric stretching mode of the COO^- groups (the band at 1407 cm^{-1} in the Raman spectrum of the solution) and a decrease of bending modes of CH_2 (the peak at 1439 cm^{-1} in the Raman spectrum of the solution) are also noticed.

Due to the well–known solvent effect, small blue shifts of the wavenumbers and the broadening of the bands were observed for the corresponding peaks in the Raman spectrum of the solution. The C–C stretching modes observed at 1002 and 942 cm^{-1} in the FT-Raman spectrum of the MSG solid state suggesting the presence of the completely ionized form of MSG [Dol74], merge to a single broad band in solution (931 cm^{-1}), with the same assignment [Eds37].

As evidenced in Figure III.6, we can show that the concentration dependent Raman spectra demonstrate the possibility to record high quality Raman spectra of MSG aqueous solution at relatively high concentration levels down to 10^{-2} M.

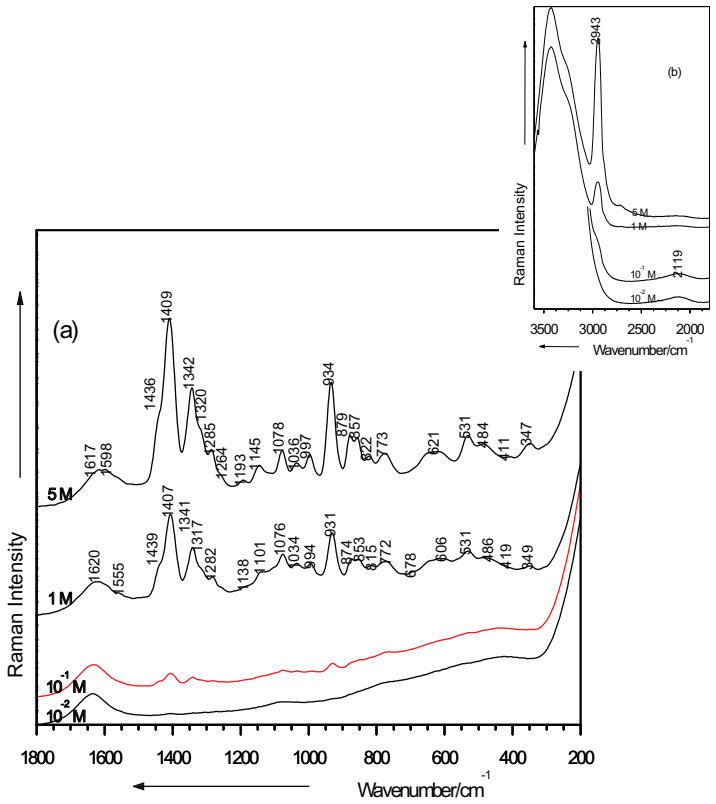

Figure III.6. Raman spectra of MSG solution at different concentrations in lower (a) and higher (b) wavenumber regions. Excitation: 514 nm, 200 mW

III.5 Raman spectra of MSG solutions at different pH values

The Raman spectra of MSG solutions at different basic pH values (Figure III.7) show no major changes for different basic pH values.

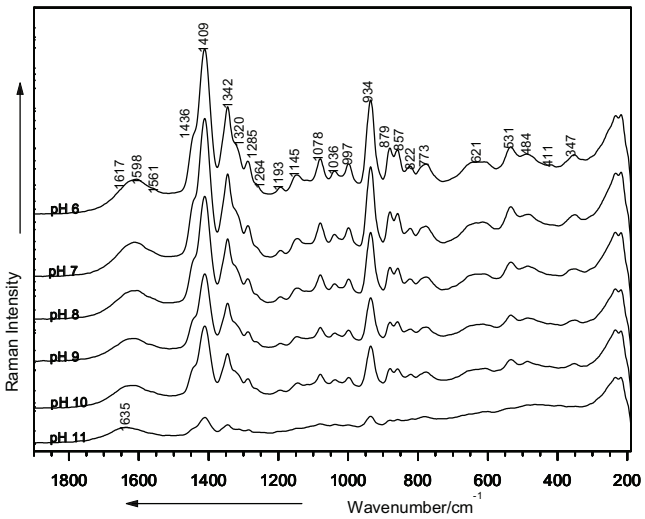

Figure III.7. Raman spectra of 5 M MSG solution at different basic pH values. Excitation: 514.5 nm, 200 mW.

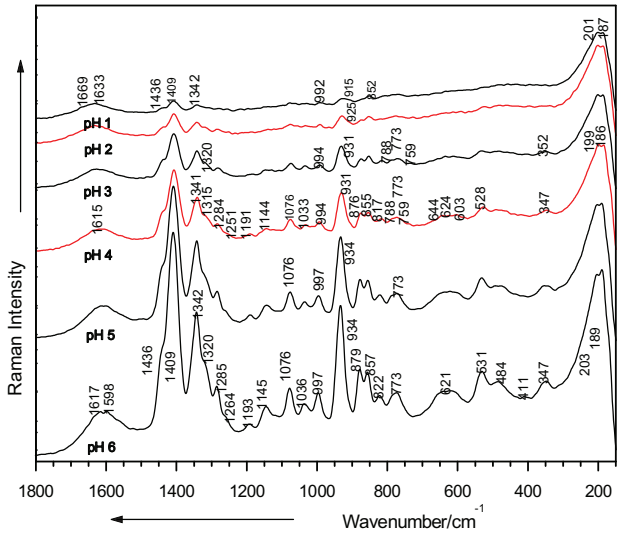

Figure III.8. Raman spectra of 5 M MSG solution at different acidic pH values. Excitation: 514.5 nm, 200 mW.

Raman spectra of MSG molecule in solution for acid pH values (Figure III.8.) show the shift of ν(C-C) stretching vibration from 934 cm^{-1} to 931 cm^{-1} and then to 915 cm^{-1} for pH=4.2 and 2 respectively. This fact shows the protonation of carboxyl group from the radical structure, and aminoacid structure respectively. For low values of pH the protonated form of MSG is prevalent.

III.6 SERS spectrum of MSG

A SERS spectrum of MSG (9.9 10^{-4} M) is presented in Figure III.9. compared to the Raman spectrum of the bulk solution (1 M) at pH=6. Large differences in band positions and relative intensities are observed, allowing the presumption of chemisorbed species.

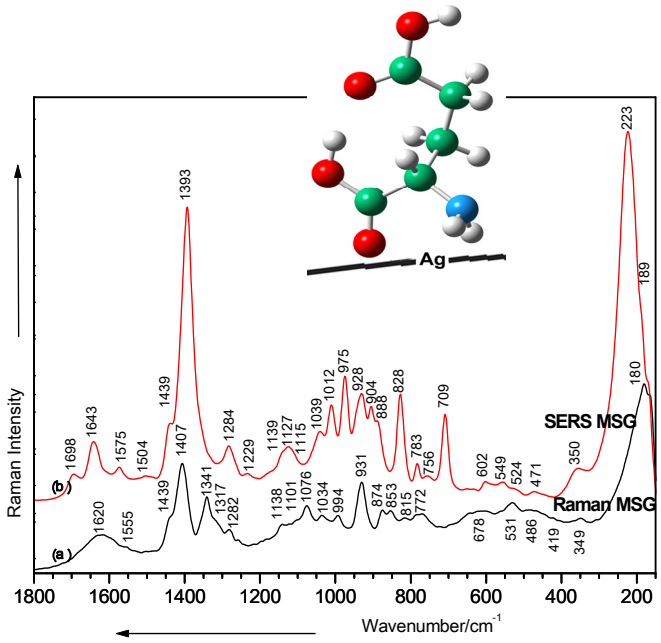

Figure III.9. Comparison between Raman (a) and SERS (b) spectra of MSG (pH 6), and its proposed orientation on the silver surface. Excitation: 514.5 nm, 200

Because the characteristic bands of the carboxylate ν(COO^-) group and the ν(C-C) bands are amplified, we propose an adsorbtion geometry perpendicular to the Ag surface. The MSG molecule binds to the silver colloidal surface through the lone pair electrons of the nitrogen atom

and the oxygens of the carboxyl group. This assumption is supported by the Ag-O [Sho02] and Ag-N [Mor99] stretching modes, which can be detected at 223 and 350 cm^{-1}, respectively.

III.7 SERS spectra at different concentrations

SERS spectra of the MSG molecule at different concentrations were performed (Figure III.10). The SERS detection limit was $6.6x10^{-5}$ M.

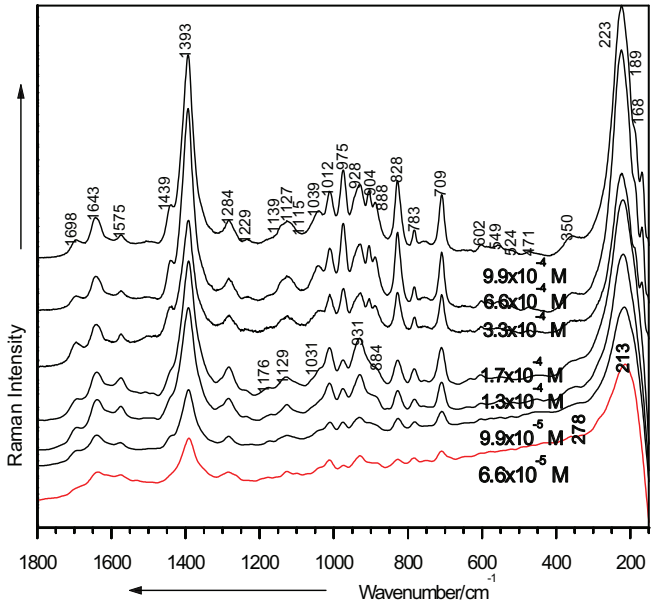

Figure III.10. SERS spectra of MSG at different concentrations. Excitation: 514.5 nm, 200mW.

III.8 SERS spectra of MSG at different basic pH values

In the SERS spectrum of MSG at pH=7 the forms and intensities of the bands at 1011, 975 and 929 cm^{-1} change, suggesting the deprotonation of the molecule (Figure III.11). The medium band at 1643 cm^{-1}, which is due to the asymmetrical bending mode of the NH_3^+ group, increases in relative intensity on going to basic pH values.

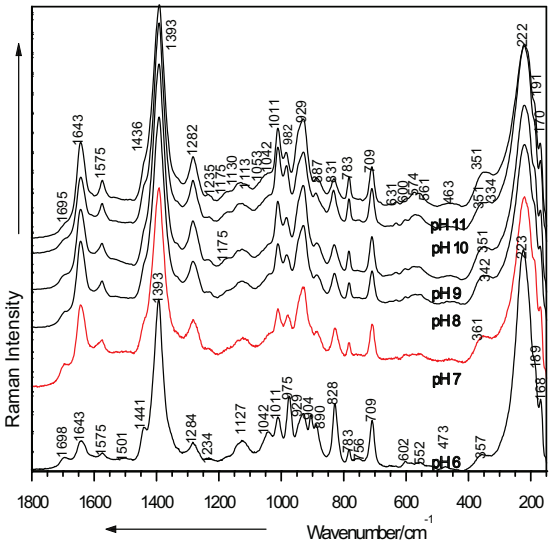

Figure III.11. SERS spectra of MSG at different basic pH values. Excitation: 514.5 nm, 200 mW.

CONCLUSIONS

Raman and SERS spectra of MSG were recorded at different concentrations.

The results extracted from FT-Raman spectrum are consistent with the zwitterionic structure of MSG in the solid state.

The geometry of MSG was computed and optimized for the first time with the BPW91/6-311++G**, BPW91/LANL2DZ, B3LYP/6-311++G**, and B3LYP/LANL2DZ methods. The two forms of MSG (monohydrate and anhydrous) possess different geometries that can be explained by the molecule protonation possibilities.

The analysis of Raman and SERS spectra of the solutions could evidence three changes in the molecular identity of MSG on going from basic to acid pH values. The quantitatively protonated form of MSG dominates at low pH values.

The SERS spectra of MSG were recorded even at very low concentrations down to 10^{-5} M.

A strong chemical interaction of MSG with the colloidal particles was observed, involving an adsorption through the lone pairs of the nitrogen atom and the oxygen atoms of the carboxyl group.

Chapter IV. Physico-chemical characterization of bixin and norbixin molecule (annatto) – E 160b

Several carotenoids are detected in the annatto seeds, the most important ones being bixin and norbixin.

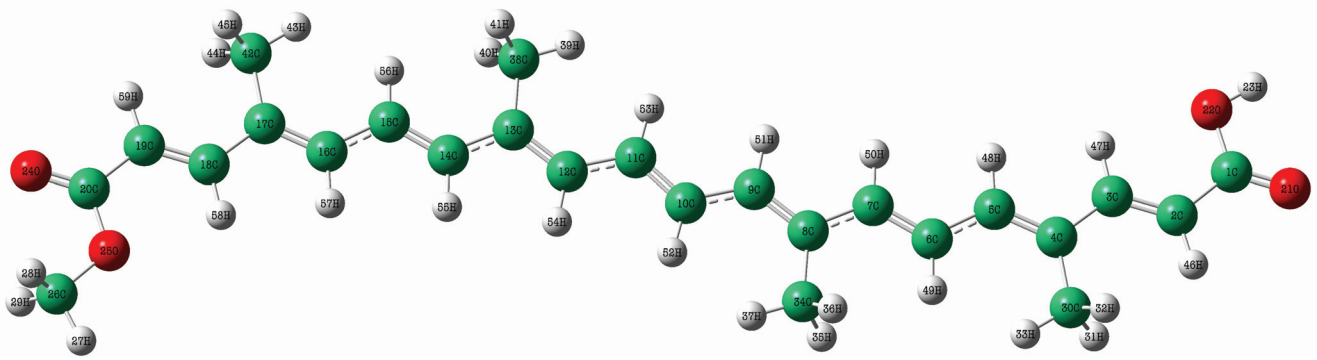

a)

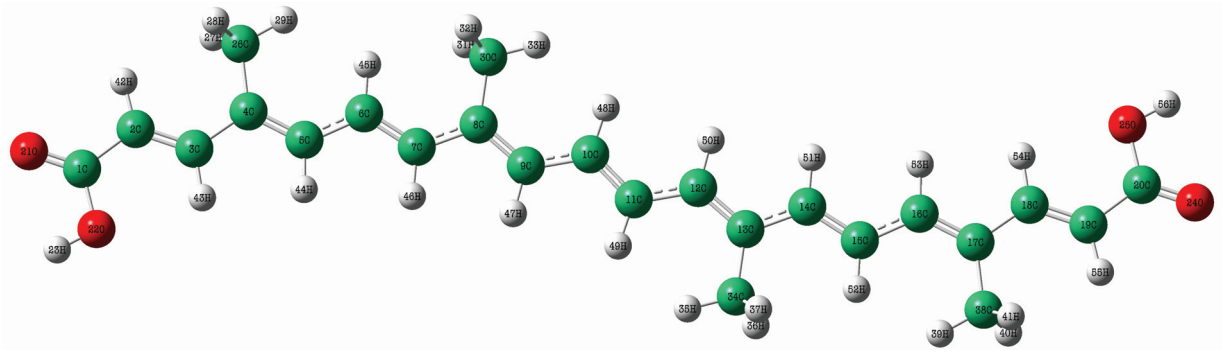

b)

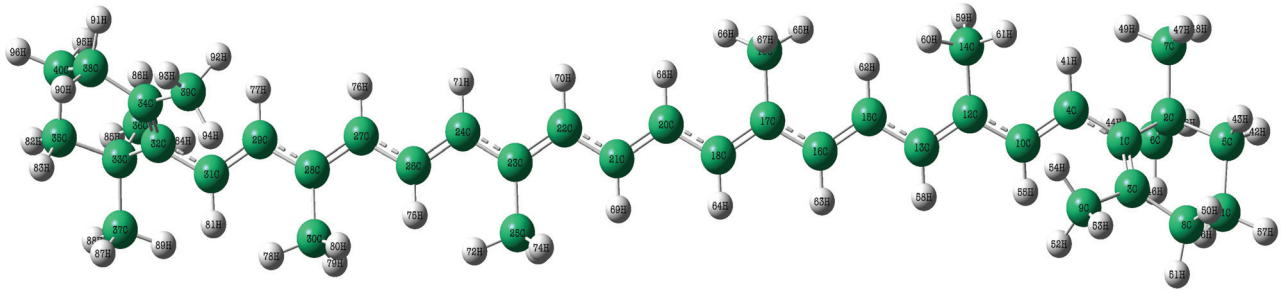

c)

Figure IV.1. The molecular geometry optimization of bixin (a), norbixin (b) and β-carotene (c).

The carotenoid bixin represents more than 80% of the total carotenoids [Dia11, Pre80, Bal06, Rib05, Góm10]. Annatto and its derivatives are members of carotenoids with long-chain conjugated polyenes, which are widely used as food additives.

IV.1 Experimental and theoretical methods

The chemicals used were: silver coloid hydroxilamine, which was prepared according to procedures described in literature [Leo03], 99.6% purity ethanol, distilled water, bixin (4.2 %) and norbixin (2.5 %). The pH was adjusted by adding HCl or NaOH solutions (10^{-1} M), respectively.

SERS spectra were recorded using a DeltaNu Advantage 532 Raman spectrometer (DeltaNu, Laramie, WY) equipped with a doubled frequency NdYAG laser emitting at 532 nm, and a USB microscope attachment (Nuscope™). The laser power was 14 mW and the spectral resolution of 10 cm^{-1}.

The molecular geometry optimizations and theoretical frecquencies were performed with the Gaussian 03 [Gau03] program by using DFT calculations with B3LYP functionals.

IV.2 Geometry Optimization

The molecular geometry optimizations of bixin and norbixin (Figure IV.1. a and b), harmonic frecquencies and electrostatic potentials (MEP) (Figure IV.6 and IV.7.) were performed by using DFT calculations.

Molecular electrostatic potentials were used to interpret and predict the reactive behaviour for a variety of chemical systems both in electrophylic and in nucleophilic reactions, for biological recognition processes and for the study of interaction trough hydrogen bonds [Pol91]. For molecules bixin and norbixin, molecular electrostatic potentials V(r) presents the most negative values in the region of atoms O21 and O24 (see Figure IV.1.a and b for atom numbering scheme) and these values are around -0.11043 a.u respectively –0.10369 a.u.. The most positive values of the molecular electrostatic potentials V(r) for these two molecules are associated around H23 for bixin and H23 and H56 for norbixin. These values are around 0.12922 a.u. for bixin and 0.12880 a.u. for norbixin.

IV.3 Raman spectra of bixin and norbixin

Figure IV.2. presents the Raman spectra of bixin and norbixin. The two profiles are similar due to the similar structures of the two molecules.

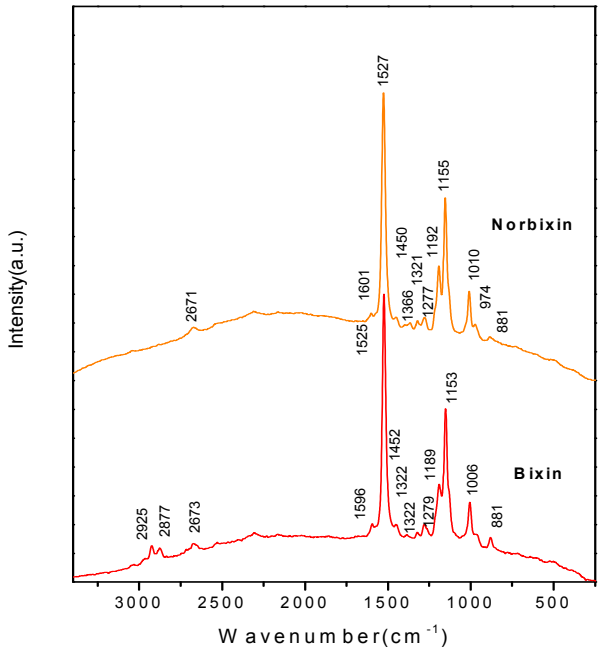

Figure IV.2. Raman spectra of bixin and norbixin. Parameters: 532 nm, 14 mW, resolution 10 cm^{-1}

By analyzing the Raman spectra one can notice the marker bands: the most intense one at 1527 cm^{-1}, assigned to the stretching vibrational mode ν(C=C) and the band at 1155 cm^{-1} assigned to the stretching vibrational mode ν(C-C) for norbixin, also the markers at 1525 cm^{-1} and 1153 cm^{-1} attributed to the vibrational stretching modes ν(C=C) and ν(C-C) for bixin.

IV.4 SERS spectra of bixin and norbixin

Figure IV.3. presents SERS spectra of bixin and norbixin which also present similar spectral profiles.

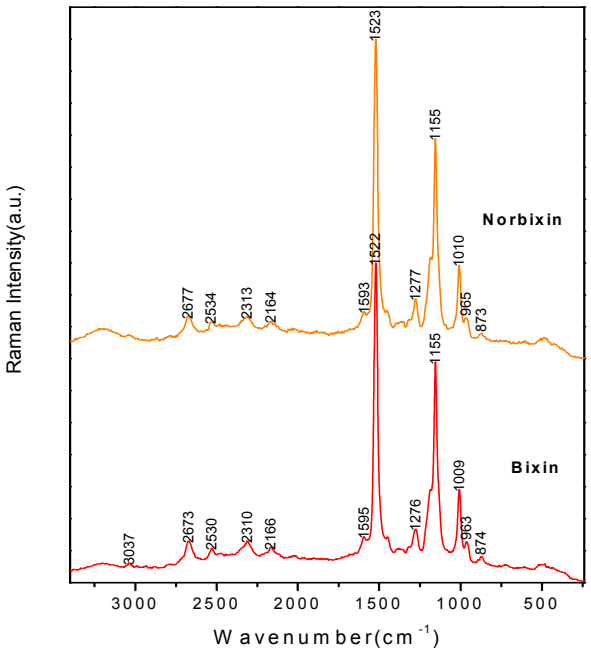

Figure IV.3. SERS spectra of bixin and norbixin. Parameters: 532 nm, 14 mW, resolution 10 cm^{-1}

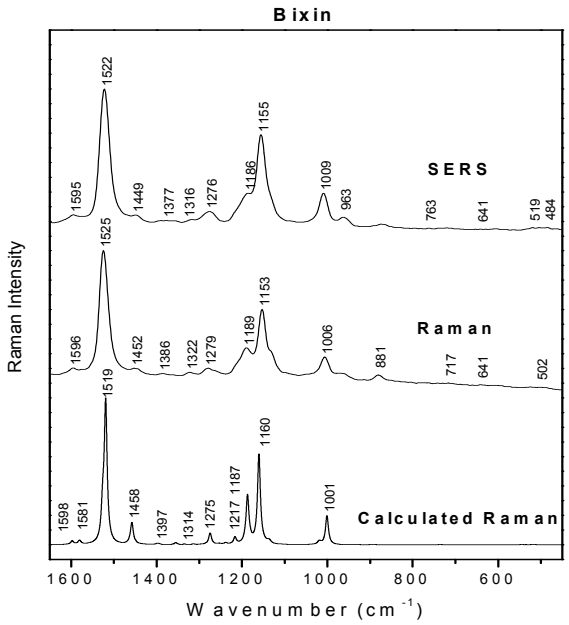

Figure IV.4. SERS, Raman and calculated Raman spectra for bixin Parameters: 532 nm, 14 mW, resolution 10 cm^{-1}

Figure IV.4. presents the compared SERS, Raman and calculated Raman spectra for bixin. There is a good correlation between the calculated and experimental Raman spectra.

A compared analysis of Raman and SERS spectra for bixin (Figure IV.4.) shows that SERS spectrum presents small changes related to the position and intensities of the bands. There are no significant differences between the Raman and SERS spectra, which demonstrates that the molecule is adsorbed, so that all the atoms of the molecule are in the near vicinity of the surface. The possibility of bixin molecule adsorbtion is made through the oxigen atoms but also through the π electrons in the carbon chain. This hypothesis is also confirmed by the calculated MEP (Figure IV.6).

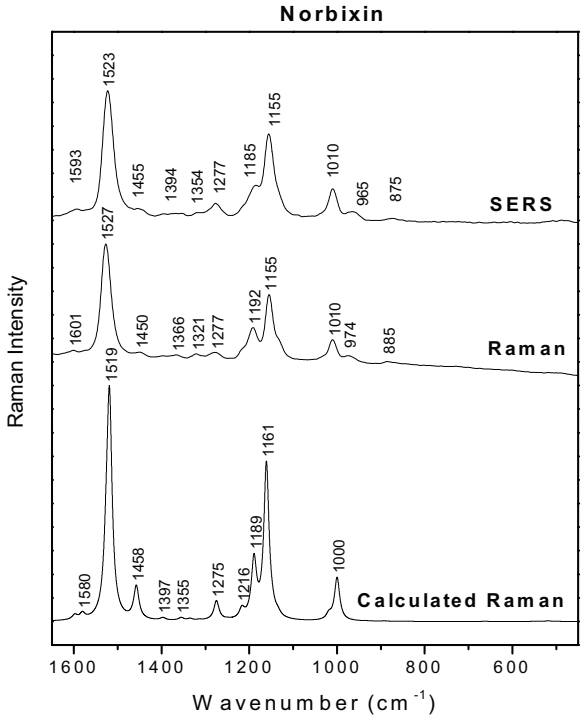

Figure IV.5. SERS, Raman and calculated Raman spectra for bixin. Parameters: 532 nm, 14mW, resolution 10 cm^{-1}

Figure IV.5. presents the SERS, Raman and Raman calculated spectra for norbixin. There is a good correlation between the calculated Raman spectrum and the experimental one. The Raman profile is also similar to the SERS profile so that, in case of norbixin, we can also assume that all the atoms of the molecule are in the near vicinity of the metallic surface. This is also an hypothesis confirmed by the calculated MEP (Figure IV.7).

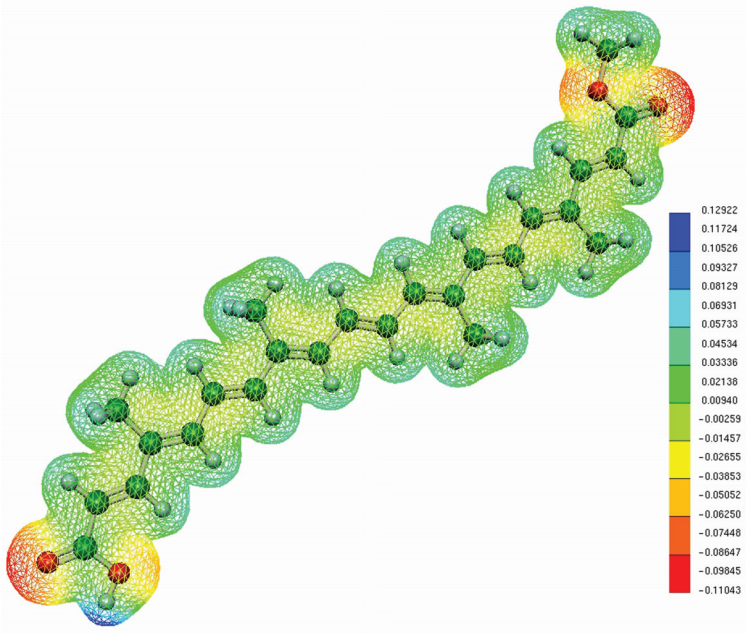

Figure IV.6. The electrostatic potential mapped on the 3D surface calculated for the bixin molecule

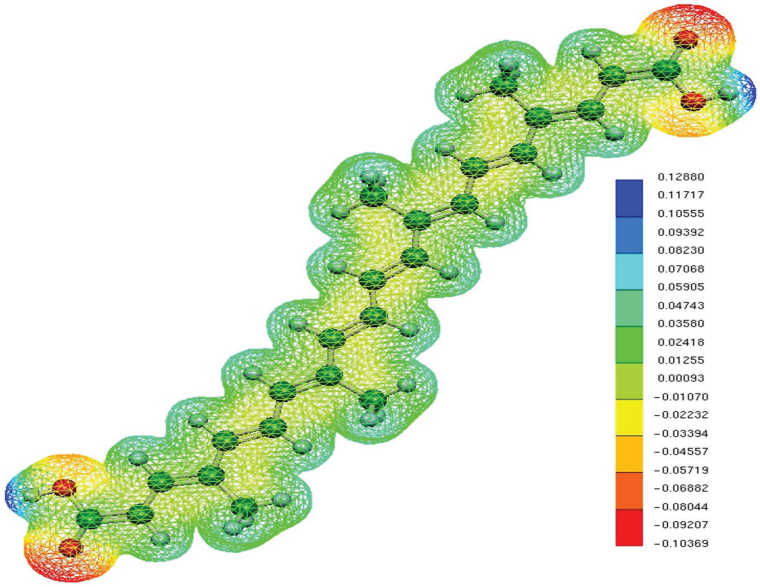

Figure IV.7. The electrostatic potential mapped on the 3D surface calculated for the norbixin molecule

IV.5 Detection of annatto food additive E160b (bixin and norbixin) in food products

By comparing the SERS spectra of bixin and norbixin with the SERS spectrum of margarine (Figure IV.8.) it can be notice a certain similarity between them, fact that indicates the presence of annatto food additive in margarine.

Based on the calibration curve UV/VIS presented in Figure IV.9, the bixine concentration in a margarine sample (0.2 g) was calculated. For the studied margarine concentration, the annatto value was 0.546 mg/100 g margarine.

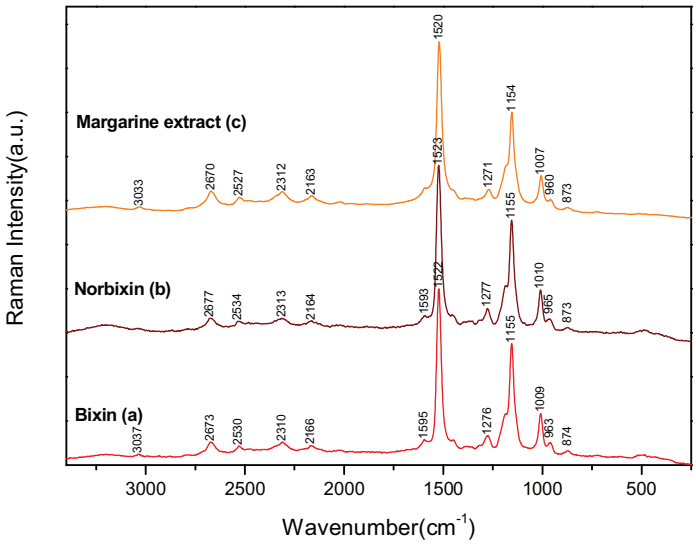

Figure IV.8. SERS spectra of bixin (a), norbixin (b) and margarine (c). Parameters: 532 nm, 14 mW, resolution 10 cm^{-1}

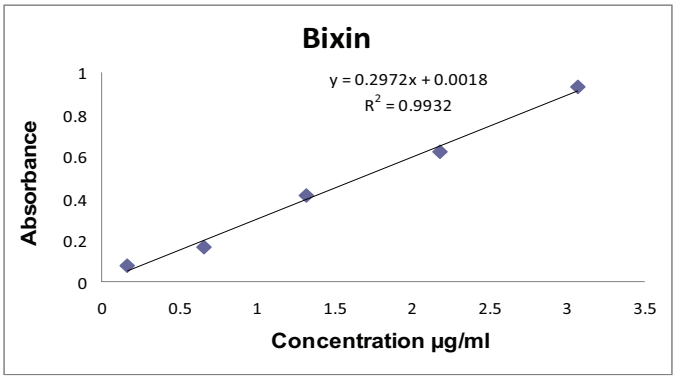

Figure IV.9. UV/VIS spectroscopy calibration curve for bixin.

The above results show that SERS spectroscopy has great potential in the qualitative evaluations, but it is difficult to use for quantitative measurements. Therefore, as a measurement technique we have employed the UV-VIS absorbtion method, which is extremely reliable for quantitative determinations but offers few qualitative informations. These two methods can be complementary used.

CONCLUSIONS

The Raman spectra of bixin and norbixin show similar profiles due to the similar structures of the two molecules.

Analyzing the Raman spectrum, the marker bands can be observed: the most intense at 1525 cm^{-1} assigned to ν(C=C) and the band at 1153 cm^{-1} assigned to ν(C-C) for bixin and the bands at 1527 cm^{-1} and 1155 cm^{-1} respectively for norbixin, for the same vibrational modes.

SERS, Raman and calculated Raman spectra for bixin are in good correlation.

The bixin and norbixin molecules are adsorbed so that all the atoms of the molecules are in the near vicinity of the surface. The possibility of bixin and norbixin molecules adsorbtion is made through the oxygen atoms but also through the π electrons in the carbon chain.

In addition the SERS spectroscopy, UV-VIS spectroscopy was also used to estimate the annatto concentration in a margarine sample; the estimated value was 0.546 g annatto/100 g margarine.

Raman and SERS spectra can serve as further references for other spectroscopic Raman applications in food analysis.

FINAL CONCLUSIONS

- This thesis presents the results of the study made on three substances of great interest in the food industry using vibrational spectroscopy: sodium benzoate E 211, monosodium glutamate E 621, annatto extract E 160b.

- By using DFT methods the molecular structure, geometry optimization and vibrational wave numbers of all these three substances were investigated. There is a good correlation between the theoretical values and the experimental ones.

- The geometry of monosodium glutamate MSG was computed and optimized for the first time with the BPW91/6-311++G**, BPW91/LANL2DZ, B3LYP/6-311++G**, and B3LYP/LANL2DZ methods. We demonstrated that both MSG forms (monohydrate and anhydrous) possess different geometries that can be explained by the molecule protonation possibilities.

- FT-Raman and/or micro-Raman spectra of the pure and impure sodium benzoate show bands assigned to the carboxylate anion vibrations and to the aromatic ring vibrations.

- The results extracted from FT-Raman spectrum are consistent with the zwitterionic structure of MSG in the solid state.

- Analyzing the Raman spectrum of bixin and norbixin, the marker bands can be observed: the most intense at 1525 cm^{-1} assigned to ν(C=C) and the band at 1153 cm^{-1} assigned to ν(C-C) for bixin and the bands at 1527 cm^{-1} and 1155 cm^{-1} respectively for norbixin for the same vibrational modes.

- The major changes in the band profiles and relative intensities appear below pH=5 in the Raman spectra of the sodium benzoate. Most likely for pH=4 (pKa=4.2), anionic molecular forms of benzoate coexist in the solution with neutral molecular forms of benzoate.

- The analysis of Raman and SERS spectra of the solutions could evidence three changes in the molecular identity of MSG on going from basic to acid pH values. The quantitatively protonated form of MSG dominates at low pH values.

- A strong chemical interaction of sodium benzoate with the silver colloidal particles was observed through the lone pair electrons of the oxygen atoms of the carboxylate anion in a perpendicular orientation.

- Under micromolar concentrations a strong chemical interaction of MSG with the colloidal particles was observed, involving an adsorption through the lone pairs of nitrogen atom and oxygen atoms from carboxyl group in a perpendicular orientation.

- The bixin and norbixin molecules are adsorbed so that all the atoms of the molecules are in the near vicinity of the surface. The possibility of bixin and norbixin molecules adsorbtion is made through the oxygen atoms but also through the π electrons in the carbon chain.

- Additional to SERS spectroscopy, UV-VIS spectroscopy was used to evaluate the annatto concentration in a sample of margarine; the obtained value is 0.546 g annatto/100 g margarine.

- This thesis is an interdisciplinary approach that demonstrates the possibility of a physical-chemical characterization of food additive molecules and also of their detection in food products by using vibrational spectroscopy methods.

- This study contains a collection of 30 relevant vibrational spectra. These spectra can serve as a valuable database reference in the interpretation of further Raman spectra studies of food, pharmaceutical and cosmetic products.

REFERENCES

[Alv06] R. W Alves, A. A. Ulson de Souza, S. M. de Arruda, G. U de Souza P. Jauregi, *Separation and Purification in the Food Industry*, 48, 2, March, 208-213 (2006)

[Baj97] K. Bajdor, P. Koczon, E. Wieckowska, W. Lewandowski, *Int. J. of Cuantum Chem*. 62, 385 (1997)

[Bal06] K. Balaswamy, P.G. Prabhakara Rao, A. Satyanarayana, D.G. Rao, *LWT - Food Science and Technology* 39, 8, 952-956 (2006)

[Bec92] A.D. Becke, *J. Chem. Phys*. 97, 9173 (1992)

[Bec93] A.D. Becke, *J. Chem. Phys.* 98, 5648 (1993)

[Bit05] C. Bittencourt, M. P. Felicissimo, J-J. Pireaux, Laurent Hossiau, *Spectroscopyeurope*, 17, 2, 16 (2005)

[Boe90] F.J. Boerio, P.P. Hong, P.J. Clark, Y. Okamoto, Langmuir, 6, 721 (1990)

[Chi05] V. Chiş, **C. Lehene**, M. Venter, O. Cozar, M. Vasilescu, N. Leopold, *Studia Univ. Babeş- Bolyai, ser. Physica,* PIM 3, 283-290 (2005).

[Chi07] V. Chiş, M. M. Venter, **C. Lehene**, M. Vasilescu, N. Leopold, O. Cozar, *J. Opt. Adv. Mat.* 9, 788 - 794 (2007)

[Dia11] V. Dias, V. Pilla, L. Alves, *J. Fluoresc 21*, 415-421 (2011)

[Dol74] F.R. Dolish, W.G. Fateley, F.F. Bentley, *Characteristic Raman Frequencies of Organic Compounds*, John Wiley&Sons Inc., 1974

[Dun76] T. H. Dunning Jr. P. J. Hay, in: P. J. Hay, in: H. F. Schaefer (Ed.), *Modern Theoretical Chemistry*, vol. 3, Plenum, New York, 1976

[Eds37] J.T. Edsall, *J. Chem. Phys*. 5, 508-517 (1937)

[Gau03] M.J. Frisch, G.W. Trucks, H.B. Schlegel, G.E. Scuseria, M.A. Robb, J.R. Cheeseman, J.A. Montgomery Jr., T. Vreven, K.N. Kudin, J.C. Burant, J.M. Millam, S.S. Iyengar, J. Tomasi, V. Barone, B. Mennucci, M. Cossi, G. Scalmani, N. Rega, G.A. Petersson, H. Nakatsuji, M. Hada, M. Ehara, K. Toyota, R. Fukuda, J. Hasegawa, M. Ishida, T. Nakajima, Y. Honda, O. Kitao, H. Nakai, M. Klene, X. Li, J.E. Knox, H.P. Hratchian, J.B. Cross, C. Adamo, J. Jaramillo, R. Gomperts, R.E.Stratmann, O. Yazyev, A.J. Austin, R. Cammi, C. Pomelli, J.W. Ochterski, P.Y. Ayala, K.Morokuma, G.A. Voth, P. Salvador, J.J. Dannenberg, V.G. Zakrzewski, S. Dapprich, A.D. Daniels, M.C. Strain, O. Farkas, D.K. Malick, A.D. Rabuck, K. Raghavachari, J.B. Foresman, J.V. Ortiz, Q. Cui, A.G. Baboul, S. Clifford, J. Cioslowski, B.B. Stefanov, G. Liu, A. Liashenko, P. Piskorz, I. Komaromi, R.L. Martin, D.J. Fox, T. Keith, M.A. Al-Laham, C.Y. Peng, A. Nanayakkara, M. Challacombe, P.M.W. Gill, B. Johnson, W. Chen, M.W. Wong, C. Gonzalez, J.A. Pople, Gaussian 03 Inc., Pittsburgh PA, (revision B.04) (2003)

[Góm10] N. M. Gómez-Ortíz, I. A. Vázquez-Maldonado, A R. Pérez-Espadas, G. J. Mena-Rejón, J. A. Azamar-Barrios, G. Oskam, *Sol. Energy Mater. Sol. Cells* 94, 40–44 (2010)

[Ior08] A. Iordache, R. Minea, M. Culea, **C. Lehene,** *Chemicke Listy*, 102, 663 – 664 (2008)

[Lee82] P. C. Lee, D. Meisel, *J. Phys. Chem.* 86, 3391-3395 (1982)

[Lee88] C. Lee, W. Yang, R. G. Parr, *Phys. Rev. B*, 37, 785 (1988)

[Leo03] N. Leopold, B. Lendl, J. Phys. Chem. B, 107, 5723-5727 (2003)

[Leo04] N. Leopold, S. Cînta-Pînzaru, M. Baia, **C. Lehene**, O. Cozar, W. Kiefer, *Studia Univ. Babeş-Bolyai, ser. Physica*, 49(1), 9-19 (2004)

[Mor99] B. Morzyc-Ociepa, D. Michalska, *Spectrochim. Acta A* 55, 2671-2676 (1999)

[Pei07] N. Peica, **C. Lehene**, N. Leopold, S. Schlücker, W. Kiefer, *Spectrochim. Acta A* 66, 604-615 (2007)

[Peic07] N. Peica, **C. Lehene**, N. Leopold, O. Cozar, W. Kiefer, *J. Opt. Adv. Mat*. 9, 9, 2943-2948 (2007)

[Per91] J. P. Perdew in : P. Ziesche, H. Eschrig (Eds.) *Electronic Structure of Solids*, Akademie Verlag, Berlin, 1991

[Per92] J. P. Perdew, Y. Wang, R. G. Parr., *Phys. Rev. B* 45, 13244 (1992)

[Pre80] H. D. Preston, M. D. Rickard, *Food Chem* 5, 47–56 (1980)

[Pol91] P. Politzer, J. S. Murray, in: *Theoretical Biochemistry and Molecular Biophysics: A Comprehensive Survey*, Vol. 2, 13. Electrostatic Potential Analysis of Dibenzo–p–dioxins and Structurally Similar Systems in Relation to Their Biological Activities Protein. D. L. Beveridge, R. Lavery, Eds., Adenine Press, Schenectady, NY 1991

[Ram10] S. Ramamoorthy, F. P. Doss, K. Kundu, V. S. V. Satyanarayana, V. Kumar, *Industrial Crops and Product*, 32, 1, 48-53 (2010)

[Rib05] J. A. Ribeiro, D. T. Oliveira, M. L. Passos, M. A. S Barrozo, *J. Food Eng*. 66, 63–68 (2005)

[Sil08] G. F. Silva, Felix M. Gamarra, A. L. Oliviera and F. A. Cabral, Brazilian *J. Chem. Eng*. 25, 2, 419-426, (2008)

[Sho02] T. Shoeib, K.W.M. Siu, A.C. Hopkinson, J. *Phys. Chem. A* 106, 6121-6128 (2002)

[Wei84] B. Weiss, *Food Additive Safety and Evaluation,* Plenum Publishing Corporation, 221-250 (1984)

AKNOWLEDGEMENTS

I would like to express my deep gratitude to the entire Biomedical Physics Department from Babeş-Bolyai University for their support during the preparation of this thesis. I am privileged to be part of a department with people of high professional and moral qualities and I have now the opportunity to thank every one for their help.

My special gratitude goes to Professor Dr. Onuc Cozar, my scientific supervisor who gave me the opportunity to start my PhD research and encouraged me during these years.

I would like to thank Lect. Dr. Nicolae Leopold who guided my first steps in research. The endless hours spent together in interpreting and discussing all scientific results had a major influence on my vision of the entire research field.

Special thanks to Prof. Dr. Vasile Chiş for his constant help, competent advice and prompt professional response whenever I needed.

I would like also to express my gratitude to Conf. Dr. Simona Cîntă-Pînzaru, for her support, good advice and constant encouragement.

My thanks go also to Prof. Dr. Monica Culea, Prof. Dr. Viorica Simon and Prof. Dr. Leontin David for their strong and constant moral support.

Special thanks to Dr. Nicoleta Peica, Dr. Loredana Leopold and Dr. Szabo Laszlo.

Last but not least, I express my deepest gratitude to the most important persons in my life, my husband Augustin for his constant and unconditioned help, support and permanent encouragement and to my beloved daughther Maria for her love and moral support.